References

[1] T. Ohji, Porous Ceramic Materials, Handb. Adv. Ceram. Mater. Appl. Process. Prop. Second Ed. (2013) 1131–1148. https://doi.org/10.1016/B978-0-12-385469-8.00059-9.

[2] P.S. Liu, G.F. Chen, General Introduction to Porous Materials, Porous Mater. (2014) 1–20. https://doi.org/10.1016/b978-0-12-407788-1.00001-0.

[3] M.L. Sandoval, A.G. Tomba Martinez, M.A. Camerucci, Mechanical and thermal behavior of cellular mullite materials, J. Eur. Ceram. Soc. 41 (2021) 6687–6696. https://doi.org/10.1016/j.jeurceramsoc.2021.05.047.

[4] L. Yuan, Z. Liu, Z. Yan, E. Jin, C. Tian, J. Yu, Effect of mullite phase formed in situ on pore structure and properties of high-purity mullite fibrous ceramics, Ceram. Int. 48 (2022) 3578–3584. https://doi.org/10.1016/j.ceramint.2021.10.136.

[5] L. Wu, C. Li, Y. Chen, C. an Wang, Seed assisted in-situ synthesis of porous anorthite/mullite whisker ceramics by foam-freeze casting, Ceram. Int. 47 (2021) 11193–11201. https://doi.org/10.1016/j.ceramint.2020.12.244.

[6] T.T. Dele-Afolabi, M.A.A. Hanim, M. Norkhairunnisa, S. Sobri, R. Calin, Research trend in the development of macroporous ceramic components by pore forming additives from natural organic matters: A short review, Ceram. Int. 43 (2017) 1633–1649. https://doi.org/10.1016/j.ceramint.2016.10.177.

[7] Y. Chen, N. Wang, O. Ola, Y. Xia, Y. Zhu, Porous ceramics: Light in weight but heavy in energy and environment technologies, Mater. Sci. Eng. R Reports. 143 (2021) 100589. https://doi.org/10.1016/j.mser.2020.100589.

[8] A.R. Studart, U.T. Gonzenbach, E. Tervoort, L.J. Gauckler, Processing routes to macroporous ceramics: A review, J. Am. Ceram. Soc. 89 (2006) 1771–1789. https://doi.org/10.1111/j.1551-2916.2006.01044.x.

[9] T. Ohji, M. Fukushima, Macro-porous ceramics: Processing and properties, Int. Mater. Rev. 57 (2012) 115–131. https://doi.org/10.1179/1743280411Y.0000000006.

[10] M. V. Twigg, J.T. Richardson, Fundamentals and applications of structured ceramic foam catalysts, Ind. Eng. Chem. Res. 46 (2007) 4166–4177. https://doi.org/10.1021/ie061122o.

[11] T. Ayode Otitoju, P. Ugochukwu Okoye, G. Chen, Y. Li, M. Onyeka Okoye, S. Li, Advanced ceramic components: Materials, fabrication, and applications, J. Ind. Eng. Chem. 85 (2020) 34–65. https://doi.org/10.1016/j.jiec.2020.02.002.

[12] X.Y. Zhang, W.L. Huo, F. Qi, Y.N. Qu, J. Xu, K. Gan, N. Ma, J.L. Yang, Ultralight Silicon Nitride Ceramic Foams from Foams Stabilized by Partially Hydrophobic Particles, J. Am. Ceram. Soc. 99 (2016) 2920–2926. https://doi.org/10.1111/jace.14320.

[13] F. Tang, H. Fudouzi, Y. Sakka, Fabrication of macroporous alumina with tailored porosity, J. Am. Ceram. Soc. 86 (2003) 2050–2054. https://doi.org/10.1111/j.1151-2916.2003.tb03607.x.

[14] I. Nettleship, Applications of porous ceramics, Key Eng. Mater. (1996) 305–324. https://doi.org/10.4028/www.scientific.net/kem.122-124.305.

[15] R. Liu, T. Xu, C. an Wang, A review of fabrication strategies and applications of porous

ceramics prepared by freeze-casting method, Ceram. Int. 42 (2016) 2907–2925. https://doi.org/10.1016/j.ceramint.2015.10.148.

[16] S. Li, J. Baeyens, R. Dewil, L. Appels, H. Zhang, Y. Deng, Advances in rigid porous high temperature filters, Renew. Sustain. Energy Rev. 139 (2021) 110713. https://doi.org/10.1016/j.rser.2021.110713.

[17] A. Gharehghani, K. Ghasemi, M. Siavashi, S. Mehranfar, Applications of porous materials in combustion systems: A comprehensive and state-of-the-art review, Fuel. 304 (2021) 121411. https://doi.org/10.1016/j.fuel.2021.121411.

[18] Z. Cuo, J. Zhang, B. Yu, S. Peng, H. Liu, Y. Chen, Spherical Al2O3-coated mullite fibrous ceramic membrane and its applications to high-efficiency gas filtration, Sep. Purif. Technol. 215 (2019) 368–377. https://doi.org/10.1016/j.seppur.2019.01.026.

[19] B. Dong, Z. Min, L. Guan, X. Zheng, L. Wang, Q. Wang, C. Yin, Y. Wang, R. Zhang, F. Wang, H. Abadikhah, X. Xu, Y. Zhang, G. Wang, Porous mullite-bonded SiC filters prepared by foaming-sol-gel-tape casting for high-efficiency hot flue gas filtration, Sep. Purif. Technol. 295 (2022). https://doi.org/10.1016/j.seppur.2022.121338.

[20] M.J. Dejneka, C.L. Chapman, S.T. Misture, Strong, low thermal expansion niobate ceramics, J. Am. Ceram. Soc. 94 (2011) 2249–2261. https://doi.org/10.1111/j.1551-2916.2011.04730.x.

[21] J.K. Park, J.H. Park, J.W. Park, H.S. Kim, Y. Il Jeong, Preparation and characterization of porous cordierite pellets and use as a diesel particulate filter, Sep. Purif. Technol. 55 (2007) 321–326. https://doi.org/10.1016/j.seppur.2006.11.009.

[22] Y. Lv, H. Liu, Z. Wang, S. Liu, L. Hao, Y. Sang, D. Liu, J. Wang, R.I. Boughton, Silver nanoparticle-decorated porous ceramic composite for water treatment, J. Memb. Sci. 331 (2009) 50–56. https://doi.org/10.1016/j.memsci.2009.01.007.

[23] J.J. Simonis, A.K. Basson, Evaluation of a low-cost ceramic micro-porous filter for elimination of common disease microorganisms, Phys. Chem. Earth. 36 (2011) 1129–1134. https://doi.org/10.1016/j.pce.2011.07.064.

[24] D. Ren, J.A. Smith, Retention and transport of silver nanoparticles in a ceramic porous medium used for point-of-use water treatment, Environ. Sci. Technol. 47 (2013) 3825–3832. https://doi.org/10.1021/es4000752.

[25] H. Zhang, V. Oyanedel-Craver, Comparison of the bacterial removal performance of silver nanoparticles and a polymer based quaternary amine functiaonalized silsesquioxane coated point-of-use ceramic water filters, J. Hazard. Mater. 260 (2013) 272–277. https://doi.org/10.1016/j.jhazmat.2013.05.025.

[26] L.S. Abebe, X. Chen, M.D. Sobsey, Chitosan coagulation to improve microbial and turbidity removal by ceramicwater filtration for household drinking water treatment, Int. J. Environ. Res. Public Health. 13 (2016). https://doi.org/10.3390/ijerph13030269.

[27] H. Wu, C. Sun, Y. Huang, X. Zheng, M. Zhao, S. Gray, Y. Dong, Treatment of oily wastewaters by highly porous whisker-constructed ceramic membranes: Separation performance and fouling models, Water Res. 211 (2022) 118042. https://doi.org/10.1016/j.watres.2022.118042.

[28] S.K. Hubadillah, M.R. Jamalludin, M.H. Dzarfan Othman, Y. Iwamoto, Recent progress on low-cost ceramic membrane for water and wastewater treatment, Ceram. Int. 48

(2022) 24157–24191. https://doi.org/10.1016/j.ceramint.2022.05.255.

[29] T. Arumugham, N.J. Kaleekkal, S. Gopal, J. Nambikkattu, R. K, A.M. Aboulella, S. Ranil Wickramasinghe, F. Banat, Recent developments in porous ceramic membranes for wastewater treatment and desalination: A review, J. Environ. Manage. 293 (2021) 112925. https://doi.org/10.1016/j.jenvman.2021.112925.

[30] Z. He, Z. Lyu, Q. Gu, L. Zhang, J. Wang, Ceramic-based membranes for water and wastewater treatment, Colloids Surfaces A Physicochem. Eng. Asp. 578 (2019). https://doi.org/10.1016/j.colsurfa.2019.05.074.

[31] F.C. Patcas, G.I. Garrido, B. Kraushaar-Czarnetzki, CO oxidation over structured carriers: A comparison of ceramic foams, honeycombs and beads, Chem. Eng. Sci. 62 (2007) 3984–3990. https://doi.org/10.1016/j.ces.2007.04.039.

[32] synthesis of Porous Cordierite and Application for Mniatalyst Support 2 C, (2016).

[33] E. Vanhaecke, S. Ivanova, A. Deneuve, O. Ersen, D. Edouard, G. Winé, P. Nguyen, C. Pham, C. Pham-Huu, 1D SiC decoration of SiC macroscopic shapes for filtration devices, J. Mater. Chem. 18 (2008) 4654–4662. https://doi.org/10.1039/b806785f.

[34] L. Du, W. Liu, S. Hu, Y. Wang, J. Yang, Preparation and photocatalytic properties of macroporous honeycomb alumina ceramics used for water purification, J. Eur. Ceram. Soc. 34 (2014) 731–738. https://doi.org/10.1016/j.jeurceramsoc.2013.09.013.

[35] T. Kim, Micro methanol reformer combined with a catalytic combustor for a PEM fuel cell, Int. J. Hydrogen Energy. 34 (2009) 6790–6798. https://doi.org/10.1016/j.ijhydene.2009.06.024.

[36] Z. Wu, C. Caliot, G. Flamant, Z. Wang, Coupled radiation and flow modeling in ceramic foam volumetric solar air receivers, Sol. Energy. 85 (2011) 2374–2385. https://doi.org/10.1016/j.solener.2011.06.030.

[37] A. Lichtner, D. Roussel, D. Jauffrès, C.L. Martin, R.K. Bordia, Effect of Macropore Anisotropy on the Mechanical Response of Hierarchically Porous Ceramics, J. Am. Ceram. Soc. 99 (2016) 979–987. https://doi.org/10.1111/jace.14004.

[38] Z. Dong, Q. Zhang, W. Chen, Fabrication of highly porous chromium carbide with multiple pore structure, J. Am. Ceram. Soc. 97 (2014) 1317–1325. https://doi.org/10.1111/jace.12777.

[39] K. Schneider, R.J. Thorne, P.J. Cameron, An investigation of anode and cathode materials in photomicrobial fuel cells, Philos. Trans. R. Soc. A Math. Phys. Eng. Sci. 374 (2016). https://doi.org/10.1098/rsta.2015.0080.

[40] Z. Tu, M.J. Zachman, S. Choudhury, S. Wei, L. Ma, Y. Yang, L.F. Kourkoutis, L.A. Archer, Nanoporous Hybrid Electrolytes for High-Energy Batteries Based on Reactive Metal Anodes, Adv. Energy Mater. 7 (2017). https://doi.org/10.1002/aenm.201602367.

[41] J.I. Roscow, J. Taylor, C.R. Bowen, Manufacture and characterization of porous ferroelectrics for piezoelectric energy harvesting applications, Ferroelectrics. 498 (2016) 40–46. https://doi.org/10.1080/00150193.2016.1169154.

[42] J. Roscow, Y. Zhang, J. Taylor, C.R. Bowen, Porous ferroelectrics for energy harvesting applications, Eur. Phys. J. Spec. Top. 224 (2015) 2949–2966. https://doi.org/10.1140/epjst/e2015-02600-y.

[43] J.I. Roscow, R.W.C. Lewis, J. Taylor, C.R. Bowen, Modelling and fabrication of porous sandwich layer barium titanate with improved piezoelectric energy harvesting figures of merit, Acta Mater. 128 (2017) 207–217. https://doi.org/10.1016/j.actamat.2017.02.029.

[44] X. Yin, L. Kong, L. Zhang, L. Cheng, N. Travitzky, P. Greil, Electromagnetic properties of Si – C – N based ceramics and composites, 59 (2014). https://doi.org/10.1179/1743280414Y.0000000037.

[45] C. Liang, Z. Wang, L. Wu, X. Zhang, H. Wang, Z. Wang, Light and Strong Hierarchical Porous SiC Foam for Efficient Electromagnetic Interference Shielding and Thermal Insulation at Elevated Temperatures, ACS Appl. Mater. Interfaces. 9 (2017) 29950–29957. https://doi.org/10.1021/acsami.7b07735.

[46] M. Carlesso, R. Giacomelli, S. Günther, D. Koch, S. Kroll, S. Odenbach, K. Rezwan, Near-net-shaped porous ceramics for potential sound absorption applications at high temperatures, J. Am. Ceram. Soc. 96 (2013) 710–718. https://doi.org/10.1111/jace.12160.

[47] G. Jean, V. Sciamanna, M. Demuynck, F. Cambier, M. Gonon, Macroporous ceramics: Novel route using partial sintering of alumina-powder agglomerates obtained by spray-drying, Ceram. Int. 40 (2014) 10197–10203. https://doi.org/10.1016/j.ceramint.2014.02.089.

[48] M. Fukushima, Microstructural control of macroporous silicon carbide, J. Ceram. Soc. Japan. 121 (2013) 162–168. https://doi.org/10.2109/jcersj2.121.162.

[49] M. Hotta, H. Kita, H. Matsuura, N. Enomoto, J. Hojo, Pore-size control in porous SiC ceramics prepared by spark plasma sintering, J. Ceram. Soc. Japan. 120 (2012) 243–247. https://doi.org/10.2109/jcersj2.120.243.

[50] X. Jin, L. Dong, H. Xu, L. Liu, N. Li, X. Zhang, J. Han, Effects of porosity and pore size on mechanical and thermal properties as well as thermal shock fracture resistance of porous ZrB2-SiC ceramics, Ceram. Int. 42 (2016) 9051–9057. https://doi.org/10.1016/j.ceramint.2016.02.164.

[51] A. Kocjan, Z. Shen, Colloidal processing and partial sintering of high-performance porous zirconia nanoceramics with hierarchical heterogeneities, J. Eur. Ceram. Soc. 33 (2013) 3165–3176. https://doi.org/10.1016/j.jeurceramsoc.2013.06.004.

[52] Q. Guo, H. Xiang, X. Sun, X. Wang, Y. Zhou, Preparation of porous YB4 ceramics using a combination of in-situ borothermal reaction and high temperature partial sintering, J. Eur. Ceram. Soc. 35 (2015) 3411–3418. https://doi.org/10.1016/j.jeurceramsoc.2015.05.023.

[53] A. Kalemtas, G. Topates, H. Özcoban, H. Mandal, F. Kara, R. Janssen, Mechanical characterization of highly porous β-Si3N4 ceramics fabricated via partial sintering & starch addition, J. Eur. Ceram. Soc. 33 (2013) 1507–1515. https://doi.org/10.1016/j.jeurceramsoc.2012.10.036.

[54] L.N.R.M. Santos, J.R.S. Silva, J.M. Cartaxo, A.M. Rodrigues, G.A. Neves, R.R. Menezes, Freeze-casting applied to ceramic materials: A short review of the influence of processing parameters, Ceramica. 67 (2021) 1–13. https://doi.org/10.1590/0366-69132021673812923.

[55] C. Vakifahmetoglu, T. Semerci, G.D. Soraru, Closed porosity ceramics and glasses, J.

Am. Ceram. Soc. 103 (2020) 2941–2969. https://doi.org/10.1111/jace.16934.

[56] X. Yan, L. Yuan, Z. Liu, E. Jin, C. Tian, J. Yu, Preparation of porous mullite ceramic for high temperature flue gas filtration application by gel casting method, J. Aust. Ceram. Soc. 57 (2021) 1189–1198. https://doi.org/10.1007/s41779-021-00613-1.

[57] F. Zhang, Z. Li, M. Xu, S. Wang, N. Li, J. Yang, A review of 3D printed porous ceramics, J. Eur. Ceram. Soc. 42 (2022) 3351–3373. https://doi.org/10.1016/j.jeurceramsoc.2022.02.039.

[58] P.S. Liu, G.F. Chen, Fabricating Porous Ceramics, Porous Mater. (2014) 221–302. https://doi.org/10.1016/b978-0-12-407788-1.00005-8.

[59] F. Li, Z. Kang, X. Huang, X.G. Wang, G.J. Zhang, Preparation of zirconium carbide foam by direct foaming method, J. Eur. Ceram. Soc. 34 (2014) 3513–3520. https://doi.org/10.1016/j.jeurceramsoc.2014.05.029.

[60] A. Arranz-Otaegui, L.G. Carretero, M.N. Ramsey, D.Q. Fuller, T. Richter, Archaeobotanical evidence reveals the origins of bread 14,400 years ago in northeastern Jordan, Proc. Natl. Acad. Sci. U. S. A. 115 (2018) 7925–7930. https://doi.org/10.1073/pnas.1801071115.

[61] H.A. Rathnayake, S.B. Navaratne, C.M. Navaratne, Porous Crumb Structure of Leavened Baked Products, Int. J. Food Sci. 2018 (2018). https://doi.org/10.1155/2018/8187318.

[62] A.K. Gupta, B. Paul, A review on utilisation of coal mine overburden dump waste as underground mine filling material: A sustainable approach of mining, Int. J. Min. Miner. Eng. 6 (2015) 172–186. https://doi.org/10.1504/IJMME.2015.070380.

[63] A. Jamal, S. Sidharth, Value added constructional bricks from overburden of opencast coalmines, J. Sci. Ind. Res. (India). 67 (2008) 445–450.

[64] N. Islam, S. Rabha, K.S.V. Subramanyam, B.K. Saikia, Geochemistry and mineralogy of coal mine overburden (waste): A study towards their environmental implications, Chemosphere. 274 (2021) 129736. https://doi.org/10.1016/j.chemosphere.2021.129736.

[65] Prashant, C.N. Ghosh, P.K. Mandal, Use of crushed and washed overburden for stowing in underground mines: A case study, J. Mines, Met. Fuels. 59 (2011) 155–161.

[66] A.A. Juwarkar, H.P. Jambhulkar, Phytoremediation of coal mine spoil dump through integrated biotechnological approach, Bioresour. Technol. 99 (2008) 4732–4741. https://doi.org/10.1016/j.biortech.2007.09.060.

[67] N.K. Kundu, M.K. Ghose, Shelf life of stock-piled topsoil of an opencast coal mine, Environ. Conserv. 24 (1997) 24–30. https://doi.org/10.1017/S0376892997000064.

[68] G.E. Blight, A.B. Fourie, Catastrophe revisited - Disastrous flow failures of mine and municipal solid waste, Geotech. Geol. Eng. 23 (2005) 219–248. https://doi.org/10.1007/s10706-004-7067-y.

[69] J.R. Owen, D. Kemp, Lèbre, K. Svobodova, G. Pérez Murillo, Catastrophic tailings dam failures and disaster risk disclosure, Int. J. Disaster Risk Reduct. 42 (2020). https://doi.org/10.1016/j.ijdrr.2019.101361.

[70] B.S. Acharya, G. Kharel, Acid mine drainage from coal mining in the United States –

An overview, J. Hydrol. 588 (2020). https://doi.org/10.1016/j.jhydrol.2020.125061.

[71] R.N. Campbell, P. Lindsay, A.H. Clemens, Acid generating of waste rock and coal ash in New Zealand coal mines, Int. J. Coal Geol. 45 (2001) 163–179. https://doi.org/10.1016/S0166-5162(00)00031-8.

[72] J.H. Park, X. Li, M. Edraki, T. Baumgartl, B. Kirsch, Geochemical assessments and classification of coal mine spoils for better understanding of potential salinity issues at closure, Environ. Sci. Process. Impacts. 15 (2013) 1235–1244. https://doi.org/10.1039/c3em30672k.

[73] R.A. Zielinski, J.K. Otton, C.A. Johnson, Sources of Salinity Near a Coal Mine Spoil Pile, North-Central Colorado, J. Environ. Qual. 30 (2001) 1237–1248. https://doi.org/10.2134/jeq2001.3041237x.

[74] B.U. Choudhury, A. Malang, R. Webster, K.P. Mohapatra, B.C. Verma, M. Kumar, A. Das, M. Islam, S. Hazarika, Acid drainage from coal mining: Effect on paddy soil and productivity of rice, Sci. Total Environ. 583 (2017) 344–351. https://doi.org/10.1016/j.scitotenv.2017.01.074.

[75] M. Balapour, T. Thway, R. Rao, N. Moser, E.J. Garboczi, Y.G. Hsuan, Y. Farnam, A thermodynamics-guided framework to design lightweight aggregate from waste coal combustion fly ash, Resour. Conserv. Recycl. 178 (2022) 106050. https://doi.org/10.1016/j.resconrec.2021.106050.

[76] Y. Ding, X. Zhang, B. Wu, B. Liu, S. Zhang, Highly porous ceramics production using slags from smelting of spent automotive catalysts, Resour. Conserv. Recycl. 166 (2021) 105373. https://doi.org/10.1016/j.resconrec.2020.105373.

[77] H.X. Zhao, F.S. Zhou, A. Evelina L.M., J.L. Liu, Y. Zhou, A review on the industrial solid waste application in pelletizing additives: Composition, mechanism and process characteristics, J. Hazard. Mater. 423 (2022) 127056. https://doi.org/10.1016/j.jhazmat.2021.127056.

[78] J. Shi, Q. Li, H. Li, S. Li, J. Zhang, Y. Shi, Eco-design for recycled products: Rejuvenating mullite from coal fly ash, Resour. Conserv. Recycl. 124 (2017) 67–73. https://doi.org/10.1016/j.resconrec.2017.04.005.

[79] A. Siddika, A. Hajimohammadi, V. Sahajwalla, Stabilisation of pores in glass foam by using a modified curing-sintering process: sustainable recycling of automotive vehicles' waste glass, Resour. Conserv. Recycl. 179 (2022) 106145. https://doi.org/10.1016/j.resconrec.2021.106145.

[80] A. Yang, C.A. Wang, R. Guo, Y. Huang, Microstructure and electrical properties of porous PZT ceramics fabricated by different methods, J. Am. Ceram. Soc. 93 (2010) 1984–1990. https://doi.org/10.1111/j.1551-2916.2010.03684.x.

[81] B.K. Saikia, C.R. Ward, M.L.S. Oliveira, J.C. Hower, F. De Leao, M.N. Johnston, A. O'Bryan, A. Sharma, B.P. Baruah, L.F.O. Silva, Geochemistry and nano-mineralogy of feed coals, mine overburden, and coal-derived fly ashes from Assam (North-east India): A multi-faceted analytical approach, Int. J. Coal Geol. 137 (2015) 19–37. https://doi.org/10.1016/j.coal.2014.11.002.

[82] M.K. Verma, P. Pandey, R. Mukhopadhyay, N. De, R. Dwivedi, N.C. Karmakar, V.K. Bajaj, Chemical characterization of selected overburdens of Singrauli coalfields, Ecol.

Environ. Conserv. 22 (2016) S207–S211.

[83] L. Banerjee, S. Chawla, S. Kumar Dash, Application of geocell reinforced coal mine overburden waste as subballast in railway tracks on weak subgrade, Constr. Build. Mater. 265 (2020) 120774. https://doi.org/10.1016/j.conbuildmat.2020.120774.

[84] N.K. Srivastava, L.C. Ram, R.E. Masto, Reclamation of overburden and lowland in coal mining area with fly ash and selective plantation: A sustainable ecological approach, Ecol. Eng. 71 (2014) 479–489. https://doi.org/10.1016/j.ecoleng.2014.07.062.

[85] Dutta et al., 2017-Environmental assessment and nano-mineralogical characterization of coal, overburden and sediment from Indian coal mining acid drainage _ Elsevier Enhanced Reader.pdf, (n.d.).

[86] Y. Taha, M. Benzaazoua, R. Hakkou, M. Mansori, Coal mine wastes recycling for coal recovery and eco-friendly bricks production, Miner. Eng. 107 (2017) 123–138. https://doi.org/10.1016/j.mineng.2016.09.001.

[87] M. Amrani, Y. Taha, Y. El Haloui, M. Benzaazoua, R. Hakkou, Sustainable reuse of coal mine waste: Experimental and economic assessments for embankments and pavement layer applications in morocco, Minerals. 10 (2020) 1–17. https://doi.org/10.3390/min10100851.

[88] X. Deng, J. Wang, J. Liu, H. Zhang, F. Li, H. Duan, Preparation and characterization of porous mullite ceramics via foam- gelcasting Preparation and characterization of porous mullite ceramics, Ceram. Int. (2015) 1–9. https://doi.org/10.1016/j.ceramint.2015.03.237.

[89] T.L. Vo, W. Nash, M. Del Galdo, M. Rezania, R. Crane, M. Mousavi Nezhad, L. Ferrara, Coal mining wastes valorization as raw geomaterials in construction: A review with new perspectives, J. Clean. Prod. 336 (2022). https://doi.org/10.1016/j.jclepro.2021.130213.

[90] L. Haibin, L. Zhenling, Recycling utilization patterns of coal mining waste in China, Resour. Conserv. Recycl. 54 (2010) 1331–1340. https://doi.org/10.1016/j.resconrec.2010.05.005.

[91] O. Santoliquido, P. Colombo, A. Ortona, Additive Manufacturing of ceramic components by Digital Light Processing: A comparison between the “bottom-up” and the “top-down” approaches, J. Eur. Ceram. Soc. 39 (2019) 2140–2148. https://doi.org/10.1016/j.jeurceramsoc.2019.01.044.

[92] B.Y. Tay, J.R.G. Evans, M.J. Edirisinghe, Solid freeform fabrication of ceramics, Int. Mater. Rev. 48 (2003) 341–370. https://doi.org/10.1179/095066003225010263.

[93] L. Yin, H.X. Peng, L. Yang, B. Su, Fabrication of three-dimensional inter-connective porous ceramics via ceramic green machining and bonding, J. Eur. Ceram. Soc. 28 (2008) 531–537. https://doi.org/10.1016/j.jeurceramsoc.2007.07.006.

[94] A. Demarbaix, F. Ducobu, N. Preux, F. Petit, E. Rivière-Lorphèvre, Green ceramic machining: Influence of the cutting speed and the binder percentage on the Y-TZP behavior, J. Manuf. Mater. Process. 4 (2020) 1–10. https://doi.org/10.3390/jmmp4020050.

[95] D. Rekow, V.P. Thompson, Near-surface damage - A persistent problem in crowns obtained by computer-aided design and manufacturing, Proc. Inst. Mech. Eng. Part H J. Eng. Med. 219 (2005) 233–243. https://doi.org/10.1243/095441105X9363.

[96] F. Filser, P. Kocher, L.J. Gauckler, Net-shaping of ceramic components by direct ceramic machining, Assem. Autom. 23 (2003) 382–390. https://doi.org/10.1108/01445150310501217.

[97] 24-Green micromachining of ceramics using tungsten carbide micro-endmills _ Elsevier Enhanced Reader.pdf, (n.d.).

[98] G. Avci, O. Akhlaghi, B. Ustbas, C. Ozbay, Y.Z. Menceloglu, O. Akbulut, A PCE-based rheology modifier allows machining of solid cast green bodies of alumina, Ceram. Int. 42 (2016) 3757–3761. https://doi.org/10.1016/j.ceramint.2015.11.004.

[99] S. Dhara, B. Su, Green machining to net shape alumina ceramics prepared using different processing routes, Int. J. Appl. Ceram. Technol. 2 (2005) 262–270. https://doi.org/10.1111/j.1744-7402.2005.02021.x.

[100] B. Su, S. Dhara, L. Wang, Green ceramic machining: A top-down approach for the rapid fabrication of complex-shaped ceramics, J. Eur. Ceram. Soc. 28 (2008) 2109–2115. https://doi.org/10.1016/j.jeurceramsoc.2008.02.023.

[101] S. Dhara, R.K. Kamboj, M. Pradhan, P. Bhargava, Shape forming of ceramics via gelcasting of aqueous particulate slurries, Bull. Mater. Sci. 25 (2002) 565–568. https://doi.org/10.1007/BF02710552.

[102] D. Galusek, P. Znášik, J. Majling, Influence of cold isostatic pressing on compaction and properties of Mg-PSZ ceramics, J. Mater. Sci. Lett. 18 (1999) 1347–1351. https://doi.org/10.1023/A:1006690500585.

[103] D. Chen, L. He, S. Shang, Study on aluminum phosphate binder and related Al2O3-SiC ceramic coating, Mater. Sci. Eng. A. 348 (2003) 29–35. https://doi.org/10.1016/S0921-5093(02)00643-3.

[104] A. Kumar, K. Mohanta, D. Kumar, O. Parkash, Green properties of dry-pressed alumina compacts fabricated using sucrose as binder, Ceram. Int. 40 (2014) 6271–6277. https://doi.org/10.1016/j.ceramint.2013.11.085.

[105] V. Hopp, A.M. Alavi, D. Hahn, P. Quirmbach, Structure–property functions of inorganic chemical binders for refractories, Materials (Basel). 14 (2021). https://doi.org/10.3390/ma14164636.

[106] J. Wang, Y. Huang, J. Lu, H. Chen, Effect of binder on the structure and mechanical properties of lightweight bubble alumina ceramic, Ceram. Int. 38 (2012) 657–662. https://doi.org/10.1016/j.ceramint.2011.06.067.

[107] M.D. Crawford, J. Baumgart, M. Shoaei, W.R. Ernst, Kinetics of the dissolution of alumina in acidic solution in a flow system, AIChE J. 34 (1988) 2012–2018. https://doi.org/10.1002/aic.690341210.

[108] M.D. Franke, W.R. Ernst, A.S. Myerson, Kinetics of dissolution of alumina in acidic solution, AIChE J. 33 (1987) 267–273. https://doi.org/10.1002/aic.690330213.

[109] T. Sato, Thermal decomposition of aluminium hydroxides, J. Therm. Anal. 32 (1987) 61–70. https://doi.org/10.1007/BF01914548.

[110] G.K. Çılgı, H. Cetişli, Thermal decomposition kinetics of aluminum sulfate hydrate, J. Therm. Anal. Calorim. 98 (2009) 855–861. https://doi.org/10.1007/s10973-009-0389-5.

[111] M.A. González-Gómez, S. Belderbos, S. Yañez-Vilar, Y. Piñeiro, F. Cleeren, G. Bormans, C.M. Deroose, W. Gsell, U. Himmelreich, J. Rivas, Development of superparamagnetic nanoparticles coated with polyacrylic acid and aluminum hydroxide as an efficient contrast agent for multimodal imaging, Nanomaterials. 9 (2019). https://doi.org/10.3390/nano9111626.

[112] F. Bustanafruz, M. Jafar-Tafreshi, M. Fazli, Studies on Thermal Decomposition of Aluminium Sulfate to Produce Alumina Nano Structure, J. Nanostructures. 2 (2013) 463–468.

[113] E.M. Ginting, N. Bukit, Synthesis and characterization of alumina precursors derived from aluminum metal through electrochemical method, Indones. J. Chem. 15 (2015) 123–129. https://doi.org/10.22146/ijc.21205.

[114] S.V. Krishnan, S. Palanivelu, M.M.M. Ambalam, R. Venkatesan, M. Arivalagan, J.M. Pearce, J. Mayandi, Chemical synthesis and characterization of nano alumina, nano composite of carbon-alumina and their comparative studies, Zeitschrift Fur Phys. Chemie. 232 (2018) 1827–1842. https://doi.org/10.1515/zpch-2017-1075.

[115] J. Grandgirard, D. Poinsot, L. Krespi, J.P. Nénon, A.M. Cortesero, Costs of secondary parasitism in the facultative hyperparasitoid Pachycrepoideus dubius: Does host size matter?, Entomol. Exp. Appl. 103 (2002) 239–248. https://doi.org/10.1023/A.

[116] K.A. Matori, L.C. Wah, M. Hashim, I. Ismail, M.H. Mohd Zaid, Phase transformations of α-alumina made from waste aluminum via a precipitation technique, Int. J. Mol. Sci. 13 (2012) 16812–16821. https://doi.org/10.3390/ijms131216812.

[117] S. Dhara, P. Bhargava, A Simple Direct Casting Route to Ceramic Foams, J. Am. Ceram. Soc. 86 (2003) 1645–1650. https://doi.org/10.1111/j.1151-2916.2003.tb03534.x.

[118] M. Pradhan, P. Bhargava, Effect of sucrose on fabrication of ceramic foams from aqueous slurries, J. Am. Ceram. Soc. 88 (2005) 216–218. https://doi.org/10.1111/j.1551-2916.2004.00001.x.

[119] K. Prabhakaran, N.M. Gokhale, S.C. Sharma, R. Lal, A novel process for low-density alumina foams, J. Am. Ceram. Soc. 88 (2005) 2600–2603. https://doi.org/10.1111/j.1551-2916.2005.00446.x.

[120] M.K. Yadav, V. Pandey, K. Mohanta, V.K. Singh, A low-cost approach to develop silica doped Tricalcium Phosphate (TCP) scaffold by valorizing animal bone waste and rice husk for tissue engineering applications, Ceram. Int. 48 (2022) 25335–25345. https://doi.org/10.1016/j.ceramint.2022.05.207.

[121] P. Jana, V. Ganesan, Processing of low-density alumina foam, J. Eur. Ceram. Soc. 31 (2011) 75–78. https://doi.org/10.1016/j.jeurceramsoc.2010.07.044.

[122] R. Narasimman, K. Prabhakaran, Preparation of low density carbon foams by foaming molten sucrose using an aluminium nitrate blowing agent, Carbon N. Y. 50 (2012) 1999–2009. https://doi.org/10.1016/j.carbon.2011.12.058.

[123] K. Huang, Y. Li, Y. Zhao, S. Li, Y. Li, S. Sang, Effects of foaming temperature on the preparation and microstructure of alumina foams, Mater. Lett. 165 (2016) 19–21. https://doi.org/10.1016/j.matlet.2015.11.097.

[124] S. Vijayan, P. Wilson, K. Prabhakaran, Porosity and cell size control in alumina foam preparation by thermo-foaming of powder dispersions in molten sucrose, J. Asian

Ceram. Soc. 4 (2016) 344–350. https://doi.org/10.1016/j.jascer.2016.06.007.

[125] H. Ji, Z. Huang, X. Wu, J. Huang, K. Chen, M. Fang, Y. Liu, Preparation, microstructure, and compressive strength of carbon foams derived from sucrose and kaolinite, J. Mater. Res. 29 (2014) 1018–1025. https://doi.org/10.1557/jmr.2014.45.

[126] K. Böhme, W.D. Einicke, O. Klepel, Templated synthesis of mesoporous carbon from sucrose-the way from the silica pore filling to the carbon material, Carbon N. Y. 43 (2005) 1918–1925. https://doi.org/10.1016/j.carbon.2005.02.043.

[127] K.E. Whitener, Rapid synthesis of thin amorphous carbon films by sugar dehydration and dispersion, AIMS Mater. Sci. 3 (2016) 1309–1320. https://doi.org/10.3934/matersci.2016.4.1309.

[128] Z. Du, D. Yao, Y. Xia, K. Zuo, J. Yin, H. Liang, Y.P. Zeng, The sound absorption performance of the highly porous silica ceramics prepared using freeze casting method, J. Am. Ceram. Soc. 103 (2020) 5990–5998. https://doi.org/10.1111/jace.17300.

[129] F. Wu, Q. Yu, F. Gauvin, H.J.H. Brouwers, A facile manufacture of highly adsorptive aggregates using steel slag and porous expanded silica for phosphorus removal, Resour. Conserv. Recycl. 166 (2021) 105238. https://doi.org/10.1016/j.resconrec.2020.105238.

[130] H. Wu, T. Kawamura, S.Y. Kim, Adsorption and separation behaviors of Y(III) and Sr(II) in acid solution by a porous silica based adsorbent, Nucl. Eng. Technol. 53 (2021) 3352–3358. https://doi.org/10.1016/j.net.2021.04.009.

[131] J. Kobayashi, K. Kawamoto, N. Kobayashi, Effect of porous silica on the removal of tar components generated from waste biomass during catalytic reforming, Fuel Process. Technol. 194 (2019) 106104. https://doi.org/10.1016/j.fuproc.2019.05.027.

[132] P. Krasucka, W. Stefaniak, A. Kierys, J. Goworek, One-pot synthesis of two different highly porous silica materials, Microporous Mesoporous Mater. 221 (2016) 14–22. https://doi.org/10.1016/j.micromeso.2015.09.023.

[133] K. Jiang, Y. Wang, L. Gui, Y. Tang, Ordered porous films of organically-modified silica prepared by a two-step replicating process, Colloids Surfaces A Physicochem. Eng. Asp. 179 (2001) 237–241. https://doi.org/10.1016/s0927-7757(00)00643-9.

[134] X. Zhou, H. Xiao, J. Feng, C. Zhang, Y. Jiang, Preparation and thermal properties of paraffin/porous silica ceramic composite, Compos. Sci. Technol. 69 (2009) 1246–1249. https://doi.org/10.1016/j.compscitech.2009.02.030.

[135] E.N. Silva, M. Cantillo-Castrillon, T.M. Dantas, Y.M. Mesquita, D.A.S. Maia, M. Bastos-Neto, W.M. Barcellos, D.C.S. Azevedo, Siloxane adsorption by porous silica synthesized from residual sand of wastewater treatment, J. Environ. Chem. Eng. 9 (2021). https://doi.org/10.1016/j.jece.2020.104805.

[136] A. Bhushan, S.K. Panda, Experimental and computational correlation of fracture parameters KIc, JIc, and GIc for unimodular and bimodular graphite components, J. Nucl. Mater. 503 (2018) 205–225. https://doi.org/10.1016/j.jnucmat.2018.03.012.

[137] S. Rajpoot, R. Malik, Y.W. Kim, Effects of polysiloxane on thermal conductivity and compressive strength of porous silica ceramics, Ceram. Int. 45 (2019) 21270–21277. https://doi.org/10.1016/j.ceramint.2019.07.109.

[138] J.J. Chen, H.J. Li, X.H. Zhou, E.Z. Li, Y. Wang, Y.L. Guo, Z.S. Feng, Efficient synthesis

of hollow silica microspheres useful for porous silica ceramics, Ceram. Int. 43 (2017) 13907–13912. https://doi.org/10.1016/j.ceramint.2017.07.118.

[139] Y. Han, L. Zhou, Y. Liang, Z. Li, Y. Zhu, Fabrication and properties of silica/mullite porous ceramic by foam-gelcasting process using silicon kerf waste as raw material, Mater. Chem. Phys. 240 (2020) 122248. https://doi.org/10.1016/j.matchemphys.2019.122248.

[140] C. Matsunaga, M. Fukushima, H. Hyuga, Y. ichi Yoshizawa, Fabrication of porous silica ceramics by gelation-freezing of diatomite slurry, J. Eur. Ceram. Soc. 37 (2017) 5259–5264. https://doi.org/10.1016/j.jeurceramsoc.2017.05.001.

[141] B. Lei, K.H. Shin, I.H. Jo, Y.H. Koh, H.E. Kim, Highly porous gelatin-silica hybrid scaffolds with textured surfaces using new direct foaming/freezing technique, Mater. Chem. Phys. 145 (2014) 397–402. https://doi.org/10.1016/j.matchemphys.2013.09.057.

[142] Z. Du, D. Yao, Y. Xia, K. Zuo, J. Yin, H. Liang, Y.P. Zeng, Highly porous silica foams prepared via direct foaming with mixed surfactants and their sound absorption characteristics, Ceram. Int. 46 (2020) 12942–12947. https://doi.org/10.1016/j.ceramint.2020.02.063.

[143] Z. Sun, C. Lu, J. Fan, F. Yuan, Porous silica ceramics with closed-cell structure prepared by inactive hollow spheres for heat insulation, J. Alloys Compd. 662 (2016) 157–164. https://doi.org/10.1016/j.jallcom.2015.12.061.

[144] B.J. Saikia, G. Parthasarathy, N.C. Sarmah, Fourier transform infrared spectroscopic estimation of crystallinity in SiO2 based rocks, Bull. Mater. Sci. 31 (2008) 775–779. https://doi.org/10.1007/s12034-008-0123-0.

[145] E. Wembabazi, P.J. Mugisha, A. Ratibu, D. Wendiro, J. Kyambadde, P.C. Vuzi, Spectroscopic analysis of heterogeneous biocatalysts for biodiesel production from expired sunflower cooking oil, J. Spectrosc. 2015 (2015). https://doi.org/10.1155/2015/714396.

[146] O.G. Buzykin, S. V. Ivanov, A.A. Ionin, A.A. Kotkov, A.Y. Kozlov, Spectroscopic detection of sulfur oxides in the aircraft wake, J. Russ. Laser Res. 26 (2005) 402–426. https://doi.org/10.1007/s10946-005-0043-z.

[147] R.S. El-Tawil, S.T. El-Wakeel, A.E. Abdel-Ghany, H.A.M. Abuzeid, K.A. Selim, A.M. Hashem, Silver/quartz nanocomposite as an adsorbent for removal of mercury (II) ions from aqueous solutions, Heliyon. 5 (2019). https://doi.org/10.1016/j.heliyon.2019.e02415.

[148] K. Jurkiewicz, M. Pawlyta, A. Burian, Structure of Carbon Materials Explored by Local Transmission Electron Microscopy and Global Powder Diffraction Probes, C. 4 (2018) 68. https://doi.org/10.3390/c4040068.

[149] F. Baino, M. Ferraris, Production and characterization of ceramic foams derived from vitrified bottom ashes, Mater. Lett. 236 (2019) 281–284. https://doi.org/10.1016/j.matlet.2018.10.122.

[150] C. Ji, D. He, L. Shen, X. Zhang, Y. Wang, A. Gupta, K. Yanagisawa, N. Bao, A facile green chemistry route to porous silica foams, Mater. Lett. 119 (2014) 60–63. https://doi.org/10.1016/j.matlet.2013.12.092.

[151] H. Xu, J. Liu, A. Guo, H. Du, Z. Hou, Porous silica ceramics with relatively high strength

and novel bi-modal pore structure prepared by a TBA-based gel-casting method, Ceram. Int. 38 (2012) 1725–1729. https://doi.org/10.1016/j.ceramint.2011.09.013.

[152] V. Pandey, S.K. Panda, V.K. Singh, Alumina dissolution process to fabricate bimodal pore architecture alumina with superior green and sintered properties, J. Am. Ceram. Soc. (2023) 1–16. https://doi.org/10.1111/jace.19280.

[153] V. Pandey, M.K. Yadav, A. Gupta, K. Mohanta, S.K. Panda, V.K. Singh, Synthesis, morphological and thermomechanical characterization of light weight silica foam via reaction generated thermo-foaming process, J. Eur. Ceram. Soc. 42 (2022) 6671–6683. https://doi.org/10.1016/j.jeurceramsoc.2022.07.034.

[154] Y. Gong, D. Zou, Z. Zhong, W. Xing, High-performance mullite fibrous ceramic filter enhanced by composite sintering aids for dust-laden gas filtration, Sep. Purif. Technol. 292 (2022) 120967. https://doi.org/10.1016/j.seppur.2022.120967.

[155] L. Gong, Y. Wang, X. Cheng, R. Zhang, H. Zhang, Thermal conductivity of highly porous mullite materials, Int. J. Heat Mass Transf. 67 (2013) 253–259. https://doi.org/10.1016/j.ijheatmasstransfer.2013.08.008.

[156] J. Wei, X. Li, T. Li, W. Chua, X. Yu, W. Zhai, Journal of Materials Science & Technology Customisable sound absorption properties of functionally graded metallic foams, J. Mater. Sci. Technol. 108 (2022) 196–207. https://doi.org/10.1016/j.jmst.2021.07.056.

[157] X. Guo, Z. Zhou, G. Ma, S. Wang, S. Zhao, Q. Zhang, Effect of forming process on the integrity of pore-gradient Al 2 O 3 ceramic foams by gelcasting, 38 (2012) 713–719. https://doi.org/10.1016/j.ceramint.2011.07.062.

[158] A. Dubey, S. Jaiswal, D. Lahiri, Promises of Functionally Graded Material in Bone Regeneration : Current Trends , Properties , and Challenges, (2022). https://doi.org/10.1021/acsbiomaterials.1c01416.

[159] J. César, E. Roberto, Journal of the European Ceramic Society Original article A versatile approach for the preparation of ceramics with porosity gradient : by using manganese and tin oxides as a model, 38 (2018) 2027–2034.

[160] W. Zhou, Z. Zhang, N. Li, W. Yan, G. Ye, A new mullite foamed ceramic prepared by direct-foaming methods in parallel with a mechanical activation technique, Ceram. Int. 48 (2022) 20721–20730. https://doi.org/10.1016/j.ceramint.2022.04.053.

[161] L. Huang, H. Qin, T. Hu, J. Xie, W. Guo, P. Gao, H. Xiao, Fabrication of high permeability SiC ceramic membrane with gradient pore structure by one-step freeze-casting process, 47 (2021) 17597–17605.

[162] M. Dolores, S. Lucio, S. Kultayeva, Y. Kim, Journal of the European Ceramic Society Improved mechanical strength and thermal resistance of porous SiC ceramics with gradient pore sizes, 42 (2022) 6785–6794.

[163] M. Trofa, E. Di Maio, P. Luca, Multi-graded foams upon time-dependent exposition to blowing agent, 362 (2019) 812–817. https://doi.org/10.1016/j.cej.2019.01.077.

[164] Y.H. Hsu, I.G. Turner, A.W. Miles, Fabrication of porous bioceramics with porosity gradients similar to the bimodal structure of cortical and cancellous bone, J. Mater. Sci. Mater. Med. 18 (2007) 2251–2256. https://doi.org/10.1007/s10856-007-3126-2.

[165] S. Sobhani, S. Allan, P. Muhunthan, E. Boigne, M. Ihme, Additive Manufacturing of Tailored Macroporous Ceramic Structures for High-Temperature Applications, 2000158 (2020) 1–8. https://doi.org/10.1002/adem.202000158.

[166] B. Marques, A. Tadeu, J. António, J. Almeida, J. de Brito, Mechanical, thermal and acoustic behaviour of polymer-based composite materials produced with rice husk and expanded cork by-products, Constr. Build. Mater. 239 (2020). https://doi.org/10.1016/j.conbuildmat.2019.117851.

[167] W. Zhou, W. Yan, N. Li, Y. Li, Y. Dai, Z. Zhang, S. Ma, Fabrication of mullite-corundum foamed ceramics for thermal insulation and effect of micro-pore-foaming agent on their properties, J. Alloys Compd. 785 (2019) 1030–1037. https://doi.org/10.1016/j.jallcom.2019.01.212.

[168] J. Yang, X. Zhang, B. Zhang, F. Liu, W. Li, J. Jian, S. Zhang, J. Yang, Mullite ceramic foams with tunable pores from dual-phase sol nanoparticle-stabilized foams, J. Eur. Ceram. Soc. 42 (2022) 1703–1711. https://doi.org/10.1016/j.jeurceramsoc.2021.12.008.

[169] Z. Yang, F. Yang, S. Zhao, K. Li, J. Chen, Z. Fei, G. Chen, In-situ growth of mullite whiskers and their effect on the microstructure and properties of porous mullite ceramics with an open/closed pore structure, J. Eur. Ceram. Soc. 41 (2021) 299–308. https://doi.org/10.1016/j.jeurceramsoc.2021.09.045.

[170] B. Xia, Z. Wang, L. Gou, M. Zhang, M. Guo, Porous mullite ceramics with enhanced compressive strength from fly ash-based ceramic microspheres: Facile synthesis, structure, and performance, Ceram. Int. 48 (2022) 10472–10479. https://doi.org/10.1016/j.ceramint.2021.12.256.

[171] X. Deng, P. Ji, J. Yin, Y. Wang, C. Song, S. Li, Y. Zhang, X. Ding, S. Ran, H. Zhang, H. Deng, Fabrication and characterization of mullite-whisker-reinforced lightweight porous materials with AlF3·3H2O, Ceram. Int. 48 (2022) 14891–14898. https://doi.org/10.1016/j.ceramint.2022.02.027.

[172] G. Chen, F. Yang, S. Zhao, K. Li, J. Chen, Z. Fei, Z. Yang, Preparation of high-strength porous mullite ceramics and the effect of hollow sphere particle size on microstructure and properties, Ceram. Int. 48 (2022) 19367–19374. https://doi.org/10.1016/j.ceramint.2022.03.231.

[173] F. Wang, S. Hao, B. Dong, N. Ke, N.Z. Khan, L. Hao, L. Yin, X. Xu, S. Agathopoulos, Porous-foam mullite-bonded SiC-ceramic membranes for high-efficiency high-temperature particulate matter capture, J. Alloys Compd. 893 (2022) 162231. https://doi.org/10.1016/j.jallcom.2021.162231.

[174] A. Najafi, M. Khoeini, A. Jamshidi, Manufacturing of nano mullite-silicon carbide filters by in situ reaction bonding, Ceram. Int. 46 (2020) 15935–15942. https://doi.org/10.1016/j.ceramint.2020.03.142.

[175] J. Tian, K. Shobu, Fabrication of Silicon Carbide – Mullite Composite by Melt Infiltration, 42 (2003) 39–42.

[176] O. Ebrahimpour, C. Dubois, J. Chaouki, Fabrication of mullite-bonded porous SiC ceramics via a sol – gel assisted in situ reaction bonding, J. Eur. Ceram. Soc. 34 (2014) 237–247. https://doi.org/10.1016/j.jeurceramsoc.2013.08.028.

[177] F. Han, Z. Zhong, Y. Yang, W. Wei, F. Zhang, W. Xing, Y. Fan, Journal of the European

Ceramic Society High gas permeability of SiC porous ceramics reinforced by mullite fibers, J. Eur. Ceram. Soc. 36 (2016) 3909–3917. https://doi.org/10.1016/j.jeurceramsoc.2016.06.048.

[178] M. Liu, X. Yang, J. Guo, L. Zhang, Fabrication of SiC foam ceramics at a low sintering temperature by adding fly ash, Ceram. Int. 48 (2022) 30462–30467. https://doi.org/10.1016/j.ceramint.2022.06.326.

[179] Z. Xing, D. Xiang, Y. Ma, Journal of the European Ceramic Society Mullite rod-enhanced porous SiC ceramics prepared at low temperature from photovoltaic waste, J. Eur. Ceram. Soc. 38 (2018) 4842–4849. https://doi.org/10.1016/j.jeurceramsoc.2018.06.042.

[180] D. Das, N. Kayal, G. Antonio, D. Gonçalves, P. Filho, M. Daniel, D.M. Innocentini, Journal of the European Ceramic Society Recycling of coal fl y ash for fabrication of elongated mullite rod bonded porous SiC ceramic membrane and its application in fi ltration, 40 (2020) 2163–2172. https://doi.org/10.1016/j.jeurceramsoc.2020.01.034.

[181] W. Wang, W. Chen, H. Liu, Recycling of waste red mud for fabrication of SiC / mullite composite porous ceramics, Ceram. Int. 45 (2019) 9852–9857. https://doi.org/10.1016/j.ceramint.2019.02.024.

[182] J. Yang, X. Zhang, B. Zhang, F. Liu, W. Li, J. Jian, S. Zhang, J. Yang, Mullite ceramic foams with tunable pores from dual-phase sol nanoparticle-stabilized foams, J. Eur. Ceram. Soc. 42 (2022) 1703–1711. https://doi.org/10.1016/j.jeurceramsoc.2021.12.008.

[183] Y. Jing, X. Deng, J. Li, C. Bai, W. Jiang, Fabrication and properties of SiC / mullite composite porous ceramics, Ceram. Int. 40 (2014) 1329–1334. https://doi.org/10.1016/j.ceramint.2013.07.013.

[184] S. Ding, S. Zhu, Y. Zeng, D. Jiang, Fabrication of mullite-bonded porous silicon carbide ceramics by in situ reaction bonding, 27 (2007) 2095–2102. https://doi.org/10.1016/j.jeurceramsoc.2006.06.003.

[185] S.Z. Salleh, A. Awang Kechik, A.H. Yusoff, M.A.A. Taib, M. Mohamad Nor, M. Mohamad, T.G. Tan, A. Ali, M.N. Masri, J.J. Mohamed, S.K. Zakaria, J.G. Boon, F. Budiman, P. Ter Teo, Recycling food, agricultural, and industrial wastes as pore-forming agents for sustainable porous ceramic production: A review, J. Clean. Prod. 306 (2021). https://doi.org/10.1016/j.jclepro.2021.127264.

[186] G. Shi, T. Liu, G. Li, Z. Wang, A novel thermal insulation composite fabricated with industrial solid wastes and expanded polystyrene beads by compression method, J. Clean. Prod. 279 (2021) 123420. https://doi.org/10.1016/j.jclepro.2020.123420.

[187] V. Jittin, A. Bahurudeen, S.D. Ajinkya, Utilisation of rice husk ash for cleaner production of different construction products, J. Clean. Prod. 263 (2020) 121578. https://doi.org/10.1016/j.jclepro.2020.121578.

[188] A. Gupta, V. Pandey, M.K. Yadav, K. Mohanta, M.R. Majhi, A comparative study on physio-mechanical properties of silica compacts fabricated using rice husk ash derived amorphous and crystalline silica, Ceram. Int. 48 (2022) 35750–35758. https://doi.org/10.1016/j.ceramint.2022.07.098.

[189] A. Pattnayak, N. Madhu, A.S. Panda, M.K. Sahoo, K. Mohanta, A Comparative study on mechanical properties of Al-SiO2 composites fabricated using rice husk silica in

crystalline and amorphous form as reinforcement, Mater. Today Proc. 5 (2018) 8184–8192. https://doi.org/10.1016/j.matpr.2017.11.507.

[190] T.G. Korotkova, S.J. Ksandopulo, A.P. Donenko, S.A. Bushumov, A.S. Danilchenko, Physical properties and chemical composition of the rice husk and dust, Orient. J. Chem. 32 (2016) 3213–3219. https://doi.org/10.13005/ojc/320644.

[191] M. Sarangi, S. Bhattacharyya, R.C. Behera, Effect of temperature on morphology and phase transformations of nano-crystalline silica obtained from rice husk, Phase Transitions. 82 (2009) 377–386. https://doi.org/10.1080/01411590902978502.

[192] A.K. Mandal, H.R. Verma, O.P. Sinha, Utilization of aluminum plant's waste for production of insulation bricks, J. Clean. Prod. 162 (2017) 949–957. https://doi.org/10.1016/j.jclepro.2017.06.080.

[193] L.P. Qian, M.R. Ahmad, J.C. Lao, J.G. Dai, Recycling of red mud and flue gas residues in geopolymer aggregates (GPA) for sustainable concrete, Resour. Conserv. Recycl. 191 (2023) 106893. https://doi.org/10.1016/j.resconrec.2023.106893.

[194] X. Lan, J. Gao, X. Qu, Z. Guo, An environmental-friendly method for recovery of soluble sodium and harmless utilization of red mud: Solidification, separation, and mechanism, Resour. Conserv. Recycl. 186 (2022) 106543. https://doi.org/10.1016/j.resconrec.2022.106543.

[195] M.A. Khairul, J. Zanganeh, B. Moghtaderi, The composition, recycling and utilisation of Bayer red mud, Resour. Conserv. Recycl. 141 (2019) 483–498. https://doi.org/10.1016/j.resconrec.2018.11.006.

[196] I. Ghosh, S. Guha, R. Balasubramaniam, A.V.R. Kumar, Leaching of metals from fresh and sintered red mud, J. Hazard. Mater. 185 (2011) 662–668. https://doi.org/10.1016/j.jhazmat.2010.09.069.

[197] G. Wang, X. an Ning, X. Lu, X. Lai, H. Cai, Y. Liu, T. Zhang, Effect of sintering temperature on mineral composition and heavy metals mobility in tailings bricks, Waste Manag. 93 (2019) 112–121. https://doi.org/10.1016/j.wasman.2019.04.001.

[198] S. Liu, X. Guan, S. Zhang, Z. Dou, C. Feng, H. Zhang, S. Luo, Sintered bayer red mud based ceramic bricks: Microstructure evolution and alkalis immobilization mechanism, Ceram. Int. 43 (2017) 13004–13008. https://doi.org/10.1016/j.ceramint.2017.07.036.

Appendix- A: List of Publications

Published Papers

1. Alumina dissolution process to fabricate bimodal pore architecture alumina with superior green and sintered properties. **Vaibhav Pandey**, S. K. Panda, V. K. Singh. ***Journal of the American Ceramic Society*** (https://doi.org/10.1111/jace.19280) (2023).
2. Synthesis, Morphological and Thermomechanical Characterization of Light Weight Silica Foam via Reaction Generated Thermo-Foaming Process. **Vaibhav Pandey**, Mayank Kumar Yadav, Ashutosh Gupta, K. Mohanta, S. K. Panda, V. K. Singh. ***Journal of European Ceramic Society*.**https://doi.org/10.1016/j.jeurceramsoc.2022.07.034 (2022).
3. An economic and sustainable approach to transform aluminosilicate-richsolid waste to functionally graded composite foam forhigh-temperature applications. **Vaibhav Pandey**, Mayank Kumar Yadav, S.K. Panda, V.K. Singh. **Chemosphere** 338 (2023) 139588. https://doi.org/10.1016/j.chemosphere.2023.139588

Submitted Papers

1. Preparation and Characterization of high-strength insulating porous bricks by reusing coal mine overburden waste, red mud and rice husk. **Vaibhav Pandey**, S. K. Panda, V. K. Singh. ***Journal of Cleaner Production.***(Under Revision).

Papers in Writing

1. An economic and sustainable methodology to transform alumina rich solid wastes into high strength light weight porous composites. **Vaibhav Pandey**, S. K. Panda, V. K. Singh. ***Resources, Conservation and Recycling.***
2. Fabrication of Mullite bonded functionally graded SiC foam with gradient microstructure via one step thermo-foaming process. **Vaibhav Pandey**, Asteek Raj, Ashutosh Gupta, Gaurav Shoora, S. K. Panda, V. K. Singh, Manas Ranjan Majhi. ***Ceramics International***.

Appendix: B: Details of Characterization Techniques

1-X-ray Diffraction (XRD)

X-ray diffraction (XRD) is a sophisticated method of examining the crystal structure and interplanar spacing of materials. It relies on the constructive interference of monochromatic X-rays and a crystalline sample. This is achieved by generating a beam of X-rays from a cathode ray tube, filtering it to obtain monochromatic radiation, collimating it to concentrate the beam, and directing it towards the sample. When the conditions align with Bragg's Law (equation 1), the incident rays interacting with the sample result in constructive interference and the production of a diffracted ray:

$$n\lambda=2d \sin \theta \ldots\ldots\ldots\ldots\ldots\ldots\ldots\ldots\ldots\ldots\ldots\ldots(1)$$

Where, n is an integer value, λ represents the wavelength of X-rays, d is interplanar spacing generating the diffraction, and θ is the diffraction angle.

Bragg's law establishes a connection between the wavelength of electromagnetic radiation, the diffraction angle, and the lattice spacing in a crystal sample. The resulting diffracted X-rays are subsequently detected, processed, and quantified. To ensure coverage of all potential lattice diffraction directions resulting from the random orientation of the powdered material, the sample is scanned across a range of 2θ angles.

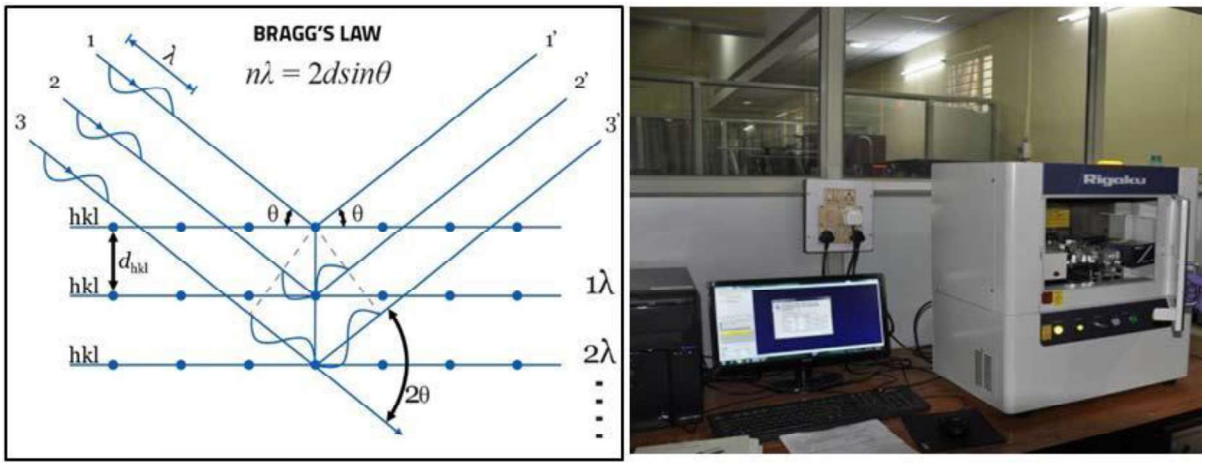

Fig. Appendix(B).0.1 Schematic representation of principle of X-Ray diffraction spectroscopy (XRD) and Photograph of XRD machine

X-ray diffractometers are comprised of three essential components: an X-ray tube, a sample holder, and an X-ray detector. In a cathode ray tube, X-rays are generated through the heating of a filament to produce electrons, accelerating these electrons towards a target by applying

voltage, and bombarding the target material with electrons. When the energy of the electrons is sufficient to displace inner shell electrons in the target material, characteristic X-ray spectra are emitted. These spectra consist of various components, with the most common ones being Kα and Kβ. Kα further includes $K_{\alpha 1}$ and $K_{\alpha 2}$, where Kα1 has a slightly shorter wavelength and twice the intensity of $K_{\alpha 2}$. The specific wavelengths depend on the target material, such as Cu, Fe, Mo, or Cr. To achieve monochromatic X-rays required for diffraction, filtration is necessary using foils or crystal monochrometers. Since Kα1 and Kα2 have closely related wavelengths, a weighted average of the two is typically used. Copper (Cu) is commonly employed as the target material for single-crystal diffraction, with CuK_{α} radiation having a wavelength of 1.5418Å. These X-rays are collimated and directed towards the sample. By rotating the sample and detector, the intensity of the reflected X-rays is recorded. When the incident X-ray geometry aligns with the Bragg Equation, constructive interference takes place, resulting in a peak in intensity. A detector captures and processes the X-ray signal, converting it into a count rate, which can be outputted to devices such as printers or computer monitors. Fig. Appendix(B).0.2provides a schematic representation and photograph of an XRD setup.

2-Scanning Electron Microscopy (SEM)

The scanning electron microscope (SEM) is utilized to examine the surface morphology of a sample at varying magnifications, resolutions, and depths of focus, offering higher resolution compared to an optical microscope. In this technique, a well-focused monoenergetic electron beam is directed onto the solid surface under investigation. The interaction between the beam and the surface leads to diverse scattering processes. Secondary electrons (SE) and backscattered electrons (BSE) are the primary signals used in SEM to capture surface morphology. These SE or BSE signals are collected and converted into current signals, which are then amplified to control the brightness of the cathode ray tube (CRT) or monitor screen. SEM operates under vacuum conditions, necessitating special sample preparation to ensure no moisture is present in the sample or chamber, as it would impede the vacuum. Conductive materials such as metals generally do not require additional preparation. However, ceramic samples are typically coated with a thin layer of gold to enhance their conductivity. In the current study, SEM analysis was conducted to examine the surface morphology of all sintered samples. The SEM instrument used was the INSPECT 50 FEI model, specifically the EVO-scanning electron microscope MA15/18 by CARL ZEISS MICROSCOPY LTD. This particular SEM is equipped with energy dispersive spectroscopy (EDX), allowing for elemental analysis

of the prepared samples through EDX and mapping techniques at specific magnifications (Fig. Appendix(B).2).

Fig. Appendix(B).2 Scanning Electron machine setup

3-Fourier Transform Infrared Spectroscopy (FTIR)

FTIR spectroscopy is a valuable technique used to identify the presence of various functional groups in both organic and inorganic molecules or compounds. It serves as a powerful tool for determining the types of chemical bonds within a molecule, generating an infrared absorption spectrum that acts as a unique "fingerprint" for the molecule. The term Fourier Transform Infrared Spectroscopy (FTIR) describes the advancement in data collection and conversion from an interference pattern to a spectrum. The method is based on the principles of the Michelson interferometer, which consists of a beam splitter, a fixed mirror, and a movable mirror that precisely moves back and forth.

During FTIR spectroscopy, radiation from a source strikes the beam splitter and separates into two beams. One beam transmits through the beam splitter and reaches the static mirror, while the other beam reflects off the beam splitter towards the moving mirror. The fixed and moving mirrors reflect the radiation back to the beam splitter. Half of the reflected radiation is transmitted, and the other half is reflected at the beam splitter. This results in one beam passing

through the sample, detected by a detector, and displayed as spectra on a computer, while the second beam returns to the radiation source.

In our study, the FTIR spectra of the samples were obtained using the "PerkinElmer Spectrum 100" instrument. The radiation sources passed through a KBr window, and the transmitted data were collected by a LiTaO3 detector. The spectra were displayed in transmitted mode. Sample pellets were prepared by mixing the sample with KBr in a ratio of 1:100. The sample pellets were then scanned in the range of 400-4000 cm-1 with a spectral resolution of 4.0 cm-1 and a scan speed of 0.2 cm/sec. Fig Appendix(B).3 provides a depiction of the working principle and a photograph of the FTIR spectrophotometer.

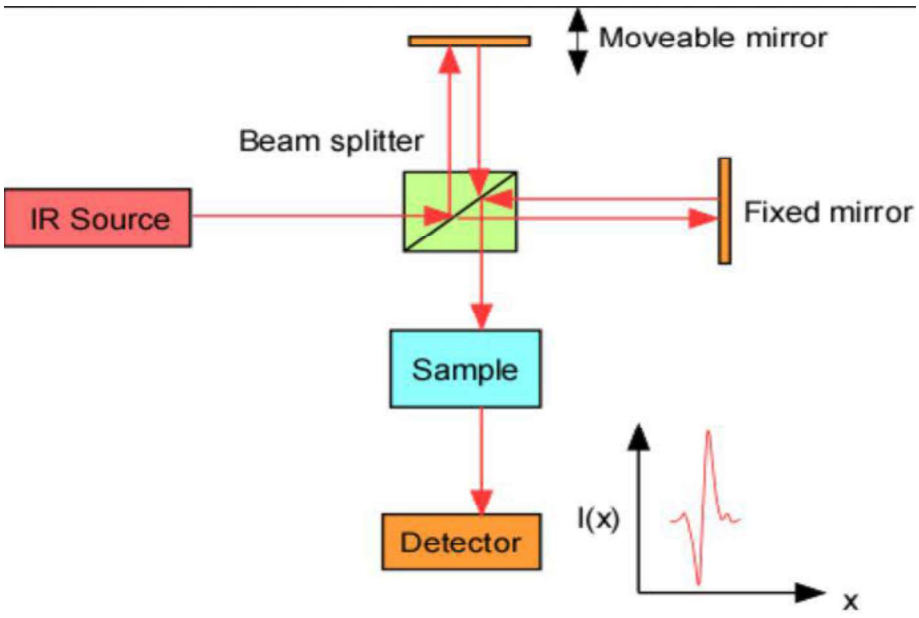

Fig. Appendix(B).0.3 Schematic representation of working of Fourier transforms infrared (FTIR) spectrophotometer and its photograph

4-Transmission Electron Microscopy (TEM)

The Transmission Electron Microscope (TEM) is a highly powerful microscope that utilizes an electron beam to focus on a specimen, producing a greatly magnified and detailed image. The magnification capability of TEM exceeds that of a light microscope by over 2 million times, enabling easy characterization of the specimen's morphological features, compositions, and crystallization information. In this technique, electrons are generated by a heated tungsten filament in the electron gun and focused onto the specimen through condenser lenses (as shown in Fig. Appendix(B).0.4). When the electrons reach the specimen, they are scattered and focused by magnetic lenses, resulting in a large, clear image. If the electrons pass through a fluorescent screen, a polychromatic image is formed. The density of the specimen determines

the extent of electron scattering, with denser specimens producing darker images due to fewer electrons reaching the screen for visualization. Conversely, thinner and more transparent specimens appear brighter.

TEM operates on similar principles as a light microscope but employs electrons instead of light. Since electrons possess both wave and particle properties, their de Broglie wavelength is significantly smaller than that of light, granting them higher resolution capabilities. This allows users of the instrument to examine fine details, down to the scale of a single column of atoms, which is tens of thousands of times smaller than the smallest resolvable object in a light microscope. TEM serves as a crucial analytical method in various scientific fields, including physical, chemical, and biological sciences. At lower magnifications, TEM images display contrast due to electron absorption in the material, as well as the thickness and composition of the specimen. At higher magnifications, complex wave interactions modulate the image intensity, necessitating expert analysis of the observed images. Alternate modes of TEM usage enable the observation of modulations in chemical identity, crystal orientation, electronic structure, sample-induced electron phase shift, in addition to regular absorption-based imaging.

In the present study, TEM analysis of the sample was performed using the TECNAI 20 G2 Electron Microscope operated at an accelerating voltage of 200 kV (as depicted in Figure 4.9). The samples were prepared by simply mounting a dilute solution of the sample on a carbon-coated TEM grid and allowing it to dry under a table lamp for 5 hours, followed by overnight vacuum drying.

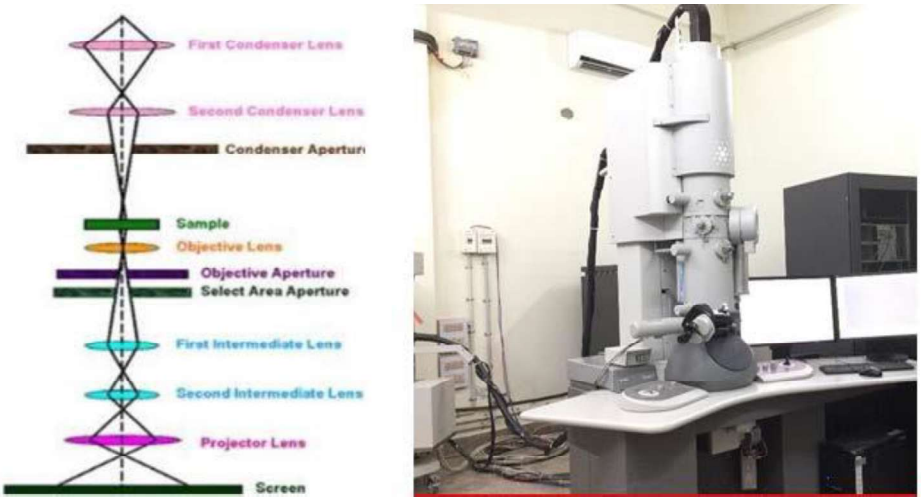

Fig. Appendix(B).0.4 Schematic representation of principle of Transmission electron microscopy (TEM) and Photograph of TEM

5-Micro computed tomography (micro-CT)

Micro computed tomography (micro-CT) is a non-destructive imaging technique that allows for the three-dimensional visualization and analysis of the internal structure of objects at a microscopic scale. It operates based on the principles of X-ray imaging and computed tomography. In micro-CT, a sample is placed on a rotating stage and exposed to a series of X-ray beams from different angles. As the X-rays pass through the sample, they interact with the material and are attenuated to varying degrees depending on the density and composition of the internal structures. The attenuated X-rays are detected by a high-resolution detector, generating a series of two-dimensional projections. These projections are then processed using mathematical algorithms to reconstruct a three-dimensional image of the internal structure of the sample. By capturing a large number of projections from different angles, micro-CT is able to provide detailed information about the spatial distribution of various materials and structures within the sample, enabling quantitative analysis, virtual slicing, and non-destructive evaluation of the sample's internal features. Micro-CT finds applications in a wide range of fields, including materials science, biomedical research, geology, archaeology, and more.

In our case, micro-computed tomography (μCT) analysis of the polished samples was conducted using the SkyScan1076 CT scanner from Aartselaar, Belgium. The specimen used had a cuboidal shape with dimensions of 15 mm in length, 10 mm in breadth, and 10 mm in height. The specimen was vertically mounted on the stage of the CT scanner. An X-ray source with a voltage of 86 kV and a current of 110 mA was employed for the analysis. During the scanning process, images were acquired at a rotation step of 0.1°. Subsequently, the obtained images were reconstructed using SkyScan's volumetric NRecon reconstruction software.

6-Thermal Conductivity

The basic principle of TPS method involves using a plane element that functions as both a temperature sensor and a heat source. This element is constructed using a thin nickel foil (10 μm) in a spiral shape, embedded in an insulating layer typically made of Kapton (70 μm thick). The temperature-sensitive (TPS) element is positioned between two samples, with the sensor faces in contact with the surfaces of the samples, as shown in Figure 1. It is important to note that two samples with similar characteristics are required for this technique.

This method offers several advantages compared to standard methods. It enables fast and straightforward experiments, providing access to a wide range of thermal conductivities ranging from 0.02 to 400 W/m K. Sample preparation requires minimal effort, and the method

offers flexibility in sample size. Additionally, by changing the diameter of the sensor, it is possible to perform localized or bulk measurements without significant adjustments.

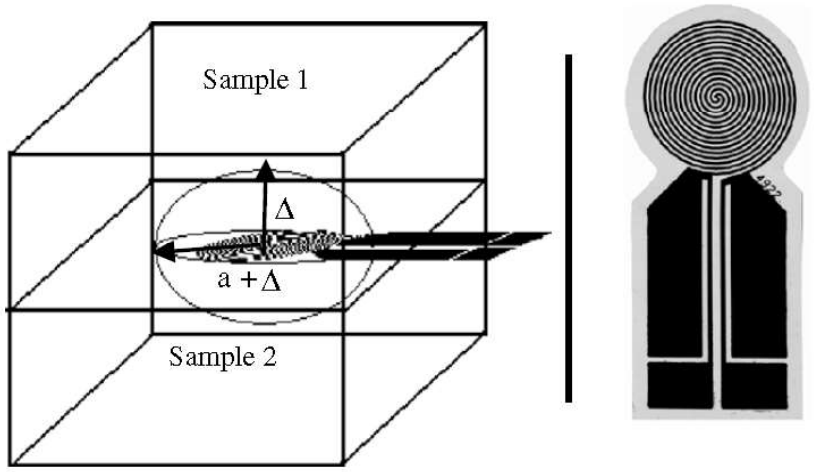

Fig. Appendix(B)0.5 Setup for TPS Measurements and Sensor Configuration

In our work, TPS-500, Goteborg, Sweden, made Hot Disk instrument has been used to measure the thermal conductivity of the porous silica. Measurements are taken by sandwiching the hot disk sensors between two identical silica foam pieces. The sensor system has an electrically conducting pattern in the shape of a double spiral laminated between two thin sheets of insulating material (Kapton).

Fig. Appendix(B)0.6 Thermal Conductivity testing setup